Non-monotonic resonance in a spatially forced Lengyel-Epstein model

Lev Haim,[1,2] Aric Hagberg,[3] and Ehud Meron[1,4]
[1]Physics Department, Ben-Gurion University of the Negev, Beer-Sheva 84105, Israel
[2]Department of Oncology, Soroka University Medical Center, Beer-Sheva 84101, Israel
[3]Center for Nonlinear Studies, Theoretical Division, Los Alamos National Laboratory, Los Alamos, New Mexico 87545, USA
[4]Department of Solar Energy and Environmental Physics, BIDR, Ben-Gurion University of the Negev, Sede Boqer Campus, Midreshet Ben-Gurion 84990, Israel

(Received 21 February 2015; accepted 12 May 2015; published online 2 June 2015)

We study resonant spatially periodic solutions of the Lengyel-Epstein model modified to describe the chlorine dioxide-iodine-malonic acid reaction under spatially periodic illumination. Using multiple-scale analysis and numerical simulations, we obtain the stability ranges of 2:1 resonant solutions, i.e., solutions with wavenumbers that are exactly half of the forcing wavenumber. We show that the width of resonant wavenumber response is a non-monotonic function of the forcing strength, and diminishes to zero at sufficiently strong forcing. We further show that strong forcing may result in a $\pi/2$ phase shift of the resonant solutions, and argue that the nonequilibrium Ising-Bloch front bifurcation can be reversed. We attribute these behaviors to an inherent property of forcing by periodic illumination, namely, the increase of the mean spatial illumination as the forcing amplitude is increased. © *2015 AIP Publishing LLC*.
[http://dx.doi.org/10.1063/1.4921768]

Spatial periodic forcing of a pattern forming system is a means of controlling spatial patterns. The degree of control that can be achieved is limited by the ability of the system to resonate with the forcing and to follow the wavenumber the forcing dictates. The common understanding is that stronger forcing leads to greater resonance ability. We use the Lengyel-Epstein (LE) model of the chlorine dioxide-iodine-malonic acid (CDIMA) reaction to show that sufficiently strong forcing may instead reduce the system's ability to resonate with the forcing. We derive this and additional results using a multiple-scale, nonlinear analysis of the model, complemented by numerical simulations. These theoretical predictions can be tested by experimental studies of the CDIMA reaction under spatially periodic illumination.

I. INTRODUCTION

The extent and the manner by which non-oscillatory pattern-forming systems can yield to an externally imposed spatial periodicity is a subject of increasing interest.[1–13] In 1D systems, this spatial resonance problem reduces to the capability of a system to adjust the actual wavenumber, k, of the pattern it forms to a fraction of an external wavenumber, k_f, provided that fraction is close enough to the wavenumber, k_0, formed by the unforced system. It is the spatial counterpart of temporally forced oscillations and shares with the latter the property of an increased yielding capability as the forcing strength is increased; the stronger the forcing, the wider the wavenumber range in which the system can lock its wavenumber to the forcing wavenumber. This property is graphically described by Arnold tongues in the plane spanned by the forcing wavenumber and the forcing strength; anywhere within the n:m resonance tongue, the system responses with a wavenumber $k = (m/n)k_f$, even though $k \neq k_0$. Arnold tongues of this kind have recently been computed for a simple spatially forced pattern formation model (the Swift-Hohenberg (SH) equation), assuming weak forcing.[6] Within any resonance tongue, the wavenumber of the pattern that the system forms is controllable by the external forcing.

In addition to increasing the controllability of the system by widening the resonance range, the forcing allows for new spatial patterns. This effect has been studied first in the context of forced oscillations,[14–19] and more recently in the context of spatial forcing of pattern-forming systems.[3,5,7,8,10] The new patterns that appear at sufficiently strong forcing are related, in part, to the multiplicity of stable phase-locked states that exist within the tongues, and to phase fronts that locally shift the phase from one state to another. In oscillatory systems, the front shifts the oscillation phase, whereas in non-oscillatory pattern-forming systems it shifts the periodic-pattern phase. Within the 2:1 resonance, an increase in the forcing strength can result in a pitchfork front bifurcation in which a pair of symmetric phase fronts that smoothly shift the phase by π clockwise and counter-clockwise merge into a single symmetric front that makes a discontinuous π shift. This nonequilibrium Ising-Bloch (NIB) bifurcation designates a transition from traveling-wave to standing-wave patterns in temporally forced oscillatory systems.[20–22] A similar front bifurcation in 2D spatially forced non-oscillatory systems[23] has been related recently to a transition from oblique to rectangular patterns.[24]

In this paper, we study the 2:1 spatial resonance in the LE model,[25] which describes the dynamics of the CDIMA reaction.[26] The motivation for this study is a recent finding

of a reversed NIB bifurcation in a spatially forced variant of the LE model.[24] We show that, unlike the picture that has emerged from earlier studies,[6,23] the effect of increasing the forcing strength is not necessarily monotonic; the resonance tongue can narrow and the NIB bifurcation can be reversed at sufficiently strong forcing.

II. LE MODEL FOR A SPATIALLY FORCED CDIMA REACTION

We use a modified 1D version of the LE model[25] that takes into account the effect of periodic illumination of the reaction cell,

$$\begin{aligned}\partial_t u &= a - u - \frac{4uv}{1+u^2} - w(x) + \partial_x^2 u\,,\\ \partial_t v &= \sigma\left[b\left(u - \frac{uv}{1+u^2} + w(x)\right) + d\partial_x^2 v\right].\end{aligned} \tag{1}$$

Here, u and v are dimensionless concentrations of iodide and chlorite ions, respectively; a, b, d, σ are dimensionless parameters, and $w(x)$ denotes the rate of the photochemical reaction, which is modulated by the spatially periodic illumination. The specific form we choose for $w(x)$ is

$$w(x) = w_0 + \frac{\gamma}{2} + p\frac{2\gamma}{\pi}\cos(k_f x)\,, \tag{2}$$

where p is a binary constant assuming the values zero or one. Equation (2) with $p=1$ represents the first and largest term in a Fourier cosine series of a square-wave forcing normally used in experiments on the CDIMA reaction.[4,24] The form (2) preserves an inherent property of forcing by periodic illumination, namely, that the spatial mean increases with the forcing amplitude. The value $p=0$ represents constant illumination with no periodic modulations.

The LE model (1) with constant forcing ($p=0$) has the stationary uniform solution

$$u_0 = \frac{a}{5} - w_0 - \frac{\gamma}{2}, \quad v_0 = \left(1+u_0^2\right)\left(\frac{w_0+\gamma/2}{u_0}+1\right). \tag{3}$$

This solution goes through a Turing bifurcation to stationary periodic patterns as b is decreased below a critical value

$$b_T = \frac{u_0 d k_T^4}{5\left(1+u_0^2\right)}\,, \tag{4}$$

where

$$k_T^2 = -5 + 2\sqrt{5}\sqrt{\frac{\left(u_0^2-1\right)v_0}{\left(u_0^2+1\right)^2}+1}\,, \tag{5}$$

and k_T is the Turing wavenumber. The stationary uniform solution also goes through a Hopf bifurcation to uniform oscillations as b is decreased below another critical value $b_H = k_T^2(k_T^2+10)(1+u_0^2)/5\sigma u_0$. To guarantee that the Turing instability is the first to be encountered as b is decreased, we chose values of a, σ, d so that $b_H < b_T$. We further focus on the 2:1 resonance, for which $k_f \approx 2k_T$.

III. NONLINEAR ANALYSIS OF THE LE MODEL

We consider the vicinity of the Turing bifurcation point b_T by introducing a small parameter, ε, which represents the deviation from b_T,

$$\varepsilon = 1 - b/b_T \ll 1\,. \tag{6}$$

We further assume weak forcing

$$\gamma = |\varepsilon|\gamma_1\,, \quad \gamma_1 \sim O(1)\,, \tag{7}$$

and introduce a small detuning parameter, ν, which represents the deviation from exact 2:1 resonance,

$$\nu = k_T - \frac{k_f}{2} = |\varepsilon|^{1/2}\nu_1\,, \quad \nu_1 \sim O(1)\,. \tag{8}$$

Near the Turing bifurcation and in the vicinity of the 2:1 resonance, where $k_f \approx 2k_T$, the solution of Eq. (1) can be approximated as

$$\begin{pmatrix} u \\ v \end{pmatrix} \approx \begin{pmatrix} u_0 \\ v_0 \end{pmatrix} + \begin{pmatrix} 1 \\ \alpha \end{pmatrix} B e^{i\frac{k_f}{2}x} + c.c.\,, \tag{9}$$

where $c.c.$ stands for the complex conjugate. Using multiple-scale analysis, we find that the amplitude B satisfies the equation

$$\tau\partial_t B = \mu B - \eta|B|^2 B + \Gamma B^\star + (\partial_x - i\nu)^2 B\,. \tag{10}$$

Further details including the derivation of Eq. (10) and the values of the coefficients in terms of the LE model (1) are given in the Appendix.

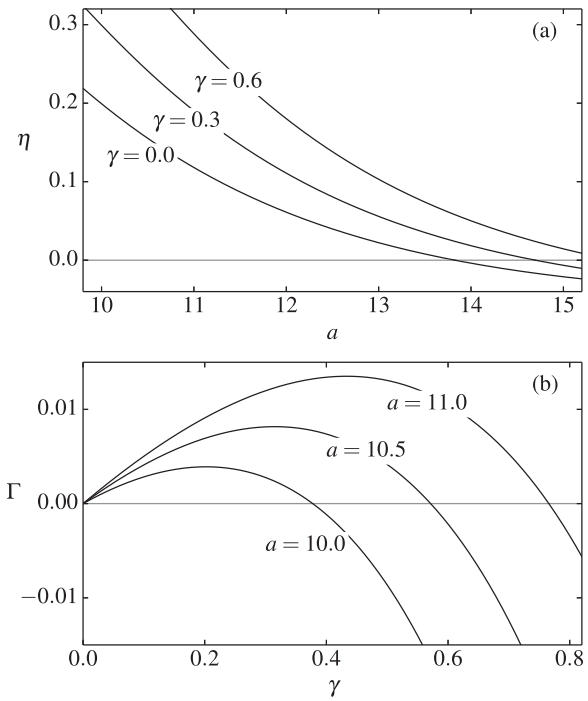

FIG. 1. The coefficients η (a) and Γ (b) of the amplitude equation (10) as functions of the LE model parameters a and γ. Note that η becomes negative at sufficiently large a values and that the dependence of Γ on γ is non-monotonic. Parameters: $k_f/k_T = 1.8$, $d=1$, $w_0=0$, and $\sigma=20$.

Figure 1(a) shows the coefficient η of the cubic term in Eq. (10) as a function of the parameter a in the LE model (1) for different values of the forcing strength γ. For a sufficiently large the parameter η becomes negative and the amplitude equation (10) is no longer valid; higher order terms should be included in the derivation to counteract the unbalanced growth of the amplitude. We therefore restrict our analysis to $\eta > 0$. Figure 1(b) shows the coefficient Γ in the amplitude equation (10) as a function of the forcing strength γ for different values of a. Surprisingly, this function is not monotonic. Moreover, Γ can assume negative values for sufficiently strong forcing.

An equation similar to Eq. (10) has been derived earlier for a spatially forced SH equation, which can be regarded as the simplest model that captures a nonuniform (finite wavenumber) stationary instability of a uniform state.[5,7] In that case, the coefficient Γ is linearly related to the forcing strength γ and the effect of the forcing is monotonic. The implications of the non-monotonic behavior found in the LE model are discussed in Sec. IV.

IV. RESONANT PATTERNS

The solution form (9) implies that stationary resonant patterns, i.e., patterns whose wavenumber is exactly $k_f/2$, correspond to constant solutions of Eq. (10). The existence range of such solutions defines the 2:1 resonance tongue. Expressing the amplitude B in terms of its modulus $\rho = |B|$ and phase $\phi = Arg(B)$, that is $B = \rho \exp(i\phi)$, such constant solutions are given by

$$\rho_0 = \sqrt{\frac{\mu - \nu^2 + \Gamma\cos(2\phi_0)}{\eta}}, \quad \text{and} \quad \phi_0 = \left\{0, \frac{\pi}{2}, \pi, \frac{3\pi}{2}\right\}. \tag{11}$$

These solutions exist for $\mu - \nu^2 + \Gamma\cos(2\phi_0) > 0$.

To study the linear stability of these solutions, we first consider the stability to uniform phase perturbations. Inserting $B = \rho\exp(i\phi)$ into Eq. (10), assuming a spatially uniform phase, we find that the equation for the phase decouples from that of the modulus and is given by $\tau\partial_t\phi = -\Gamma\sin 2\phi$. The stability of the solutions $B_0 = \rho_0\exp(i\phi_0)$ to phase perturbations is determined by the sign of the eigenvalue $\lambda = -2\Gamma\cos 2\phi_0$. It is readily seen that for $\Gamma > 0$ the solutions with $\phi_0 = \pi/2,\ 3\pi/2$ are unstable, while for $\Gamma < 0$ those with $\phi_0 = 0,\ \pi$ are unstable.

We consider now the stability of B_0 to general perturbations and write a perturbed solution as $B(x,t) = B_0 + \delta B(x,t)$, where

$$\delta B(x,t) = a_+(t)e^{iqx} + a_-^\star(t)e^{-iqx}. \tag{12}$$

Inserting this form into Eq. (10) and linearizing, we find

$$\begin{pmatrix}\dot{a}_+\\ \dot{a}_-\end{pmatrix} = \mathbf{J}\begin{pmatrix}a_+\\ a_-\end{pmatrix}, \quad \mathbf{J} = \begin{pmatrix}D_+ & C\\ C^\star & D_-\end{pmatrix}, \tag{13}$$

where $D_\pm = \mu - 2\eta|B_0|^2 - (q\mp\nu)^2$ and $C = \Gamma - \eta B_0^2$. The stability properties of the resonant solution B_0 are determined by the eigenvalues,

$$\lambda_\pm(q) = \frac{D_+ + D_-}{2} \pm \sqrt{\left(\frac{D_+ + D_-}{2}\right)^2 - D_+D_- + |C|^2}, \tag{14}$$

of the Jacobian matrix $\mathbf{J}$. To determine the stability range of the solution B_0 within its existence range, we demand that $\lambda_\pm(q) < 0$ for any given wavenumber q. The wavenumbers that maximize λ_+ are

$$q_c = \begin{cases} \pm\dfrac{\sqrt{4\nu^4 - |C|^2}}{2\nu} & \text{if } -\nu^2 < \mu < 3\nu^2, \\ 0, & \text{otherwise}, \end{cases} \tag{15}$$

where we have considered only λ_+, because $\lambda_+ > \lambda_-$. Inserting the critical wavenumbers (15) into the eigenvalue expression (14), we find the stability domains of the resonant solution in terms of the amplitude equation parameters μ, ν, and Γ and the phase of the solution B_0,

$$\begin{cases} \Gamma\cos 2\phi_0 > \dfrac{(\mu - 3\nu^2)^2}{8\nu^2} & \text{if } -\nu^2 < \mu < 3\nu^2, \\ \Gamma\cos 2\phi_0 > 0, & \text{otherwise}. \end{cases} \tag{16}$$

To connect the results of the amplitude equation stability analysis in Eq. (16) to the LE model (1), we plot the stability regions in the $(\gamma, k_f/k_T)$ parameter plane. Figure 2 shows the existence and stability ranges of the symmetric resonant periodic solutions, $B_0 = \rho_0\exp(i\phi_0),\ \phi_0 = 0, \pi$, in the forcing-parameters plane $(\gamma, k_f/k_T)$, based on the analytical results. Also shown in Fig. 2 are computational results of the stability region using direct numerical solutions of the LE model (1). The numerical and analytical results are in good agreement especially for smaller forcing and detuning. Notice that the resonance range of stable solutions first increases with the forcing strength γ, reaches a maximum and then decreases until it vanishes. This surprising behavior results from the non-monotonic dependence of Γ on γ (see Fig. 1).

For the parameters used to produce Fig. 2, the resonant solutions with phases $\phi_0 = \pi/2, 3\pi/2$ exist for sufficiently small γ, but are unstable. Figure 3 shows a similar diagram

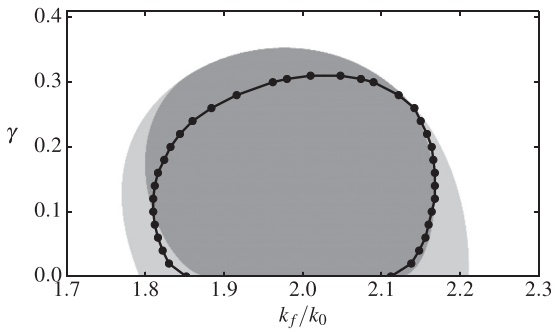

FIG. 2. Existence and stability domains of resonant solutions, B_0, of Eq. (10) with $\phi_0 = 0, \pi$. The light gray areas indicate the existence domain, while the dark gray area shows the stability region. The black curve demarcates the borders of the numerically computed stability region using the LE model (1). Parameters: $a = 10.5$, $\sigma = 20$, $d = 1$, $w_0 = 0$, and $b = 0.25$. For these parameters, the solutions with $\phi_0 = \pi/2, 3\pi/2$ are unstable.

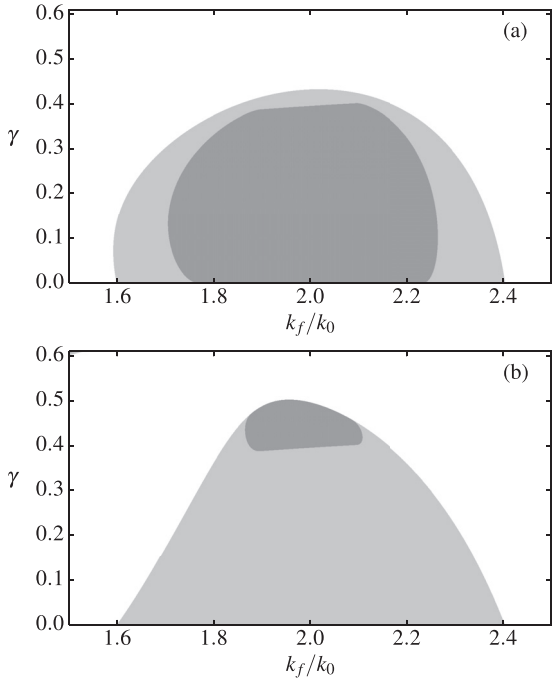

FIG. 3. Existence and stability domains of resonant solutions, B_0, of Eq. (10) for (a) $\phi_0 = 0, \pi$ solutions and (b) $\phi_0 = \pi/2, 3\pi/2$ solutions. The light gray areas indicate the existence domain, while the dark gray area shows the stability region. Parameters: $a = 10$, $\sigma = 50$, $d = 1$, $w_0 = 0$, and $b = 0.185$.

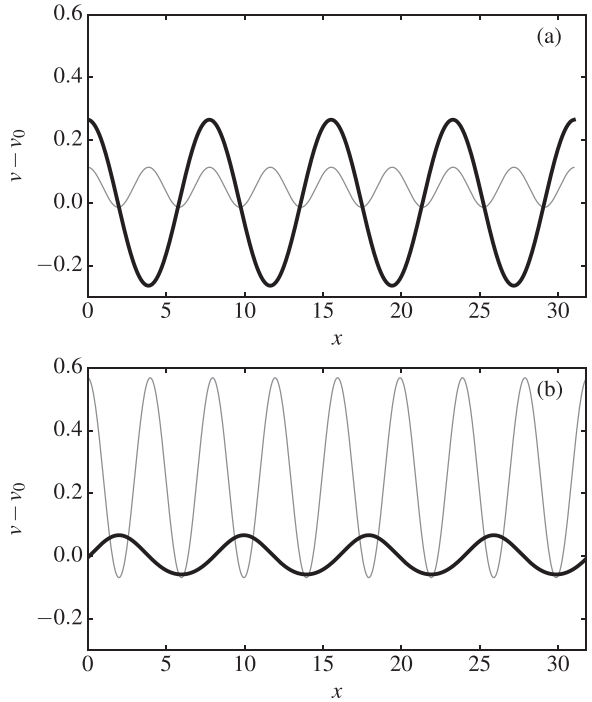

FIG. 4. The shape of periodic resonant solutions at different forcing strengths in the LE model (1). The dark curves represent the solutions $v - v_0$ and the gray curves are the forcing $w(x)$. (a) Weak forcing leads to resonant periodic solutions with phases $\phi_0 = 0, \pi$ for which maxima of the solution coincide with maxima of the forcing ($\gamma = 0.1$). (b) Strong forcing leads to resonant periodic solutions with phases $\phi_0 = \pi/2, 3\pi/2$ for which maxima of the solution coincide with minima of the forcing ($\gamma = 0.5$). Parameters: $k_f/k_T = 2$, $d = 1$, $w_0 = 0$, $b = 0.185$, $a = 10$, and $\sigma = 50$.

using a different set of LE parameters values for which the $\phi_0 = 0, \pi$ solutions (Fig. 3(a)) are stable for small γ, whereas the $\phi_0 = \pi/2, 3\pi/2$ solutions (Fig. 3(b)) become stable for sufficiently large γ values. The swap in the stability properties of the solutions is due to the change in sign of Γ as is shown in Fig. 1(b).

The spatial profiles of the resonant solutions relative to the forcing are shown in Fig. 4. The figure demonstrates that both type of solutions, that is $\phi_0 = 0, \pi$ (Fig. 4(a)) and $\pi/2$ shifted one (Fig. 4(b)), can be stable for the same unforced system parameters but with different forcing strength.

The amplitude equation (10) has stationary front solutions that are bi-asymptotic to the pair of symmetric phase solutions, $\phi_0 = 0, \pi$ for $\Gamma > 0$. These solutions go through a NIB bifurcation, from an Ising front to a pair of Bloch fronts, as Γ is decreased below a threshold value.[20] Since Γ is a non-monotonic function of the forcing strength γ, the bifurcation from Ising to Bloch fronts may occur as γ is increased. Indeed, such a reversed NIB bifurcation has been found in the forced LE model.[24]

V. DISCUSSION

The non-monotonic dependence of the coefficient Γ of the forcing term in the amplitude equation (10) on the forcing strength, represented by the parameter γ in the LE model (1), has several consequences. First, it narrows down the resonance range at high forcing strengths until it vanishes. This is a significant result when using spatial forcing to control the wavenumber of a system; stronger forcing may reduce the control capability. Second, the NIB bifurcation may be reversed, since Γ can decrease as γ is increased. Moreover, a range of γ that capture both forward and backward NIB bifurcations may be identified. Third, for sufficiently large γ, the coefficient Γ can change sign. This renders the phase solutions $\phi_0 = 0, \pi$ unstable and stabilizes the $\phi_0 = \pi/2, 3\pi/2$ solutions for which maxima of the controlled pattern correspond to minima of the forcing.

The non-monotonic dependence of Γ is related to the form of the periodic forcing; rather than oscillating about a constant mean, often taken to be zero, the mean increases with the forcing amplitude. In the present study, this form is motivated by physical grounds; the intensity of the periodic illumination is bounded below by zero and increasing its amplitude implies increasing its mean value too.

Using a spatial forcing regime with an increasing mean may result in non-monotonic behavior in other systems too. An example of such a system is a dryland landscape with restored vegetation. Vegetation restoration can be achieved by periodic soil-crust removal, which increases the infiltration rate of surface water into the soil periodically in space, and forms domains of favorable growth conditions.[13] Moreover, a similar effect may hold for temporal forcing of oscillating systems. The LE model captures also a Hopf bifurcation which accounts for oscillatory and traveling-wave dynamics in the CDIMA reaction.[26] A non-monotonic relation between Γ and γ that results in both forward and backward NIB bifurcations may lead, in such a context, to an extended range of Bloch-front turbulence,[17] a state of spatio-temporal chaos nurtured by spontaneous events of spiral-wave nucleation.[27]

ACKNOWLEDGMENTS

We wish to thank Milos Dolnik and Irving Epstein for many helpful discussions. The support of the United States-Israel Binational Science Foundation (Grant No. 2008241) is gratefully acknowledged. Part of this work was funded by the Laboratory Directed Research and Development program at Los Alamos National Laboratory under Department of Energy Contract No. DE-AC52-06NA25396.

APPENDIX: DERIVATION OF AMPLITUDE EQUATION

We describe here the derivation of the amplitude equation (10) using multiple scale analysis.[28,29] The solution that appears beyond the Turing bifurcation has the approximate form

$$\begin{pmatrix} u \\ v \end{pmatrix} \approx \begin{pmatrix} u_0 \\ v_0 \end{pmatrix} + \begin{pmatrix} 1 \\ \alpha \end{pmatrix} A(X,T)e^{ik_T x} + c.c., \tag{A1}$$

where A describes the complex-valued amplitude of the Turing mode that grows beyond the instability and α is a constant. Near the Turing bifurcation, we expect A to be small in absolute value, i.e., $|A| \ll 1$, and to vary slowly in space and time. To capture these properties of A, we define the slow variables

$$T = |\varepsilon| t, \quad X = |\varepsilon|^{1/2} x, \tag{A2}$$

so that $|\partial_t A| = \varepsilon |\partial_T A| \sim |A| \ll 1$ and $|\partial_x A| = \varepsilon^{1/2} |\partial_X A| \sim |A| \ll 1$. Using the chain rule, we transform the time and space derivatives according to

$$\partial_t \to |\varepsilon| \partial_T, \quad \partial_x \to \partial_x + |\varepsilon|^{1/2} \partial_X, \tag{A3}$$

where ∂_x acts only on fast varying factors, such as $\exp(ik_T x)$, and ∂_X and ∂_T act only on slowly varying factors that involve the amplitude A.

Expanding the solution to Eq. (1) as

$$\begin{pmatrix} u \\ v \end{pmatrix} = \begin{pmatrix} u_0 \\ v_0 \end{pmatrix} + |\varepsilon|^{1/2} \begin{pmatrix} u_1 \\ v_1 \end{pmatrix} + |\varepsilon| \begin{pmatrix} u_2 \\ v_2 \end{pmatrix} + |\varepsilon|^{3/2} \begin{pmatrix} u_3 \\ v_3 \end{pmatrix} + \dots, \tag{A4}$$

substituting all expansions into the LE model (1), and grouping terms by their order, we find at order $|\varepsilon|^{1/2}$,

$$\mathcal{L} \begin{pmatrix} u_1 \\ v_1 \end{pmatrix} = \begin{pmatrix} 4\zeta_1 - 5 + \partial_x^2 & -4\zeta_2 \\ \sigma b_T \zeta_1 & -\sigma b_T \zeta_2 + d\sigma \partial_x^2 \end{pmatrix} \begin{pmatrix} u_1 \\ v_1 \end{pmatrix} = 0, \tag{A5}$$

where

$$\zeta_1 = 1 + \left(\frac{2u_0^2}{(u_0^2+1)^2} - \frac{1}{u_0^2+1} \right) v_0, \quad \zeta_2 = \frac{u_0}{1+u_0^2}. \tag{A6}$$

We consider the operation of $\mathcal{L}$ on a vector space of periodic functions with period $L = 2\pi/k_T$ on which the following inner product between any two vector functions $\mathbf{f} = (f_1, f_2)$ and $\mathbf{g} = (g_1, g_2)$ is defined:

$$\langle f, g \rangle = \sum_{i=1,2} \int_0^L f_i^* g_i dx. \tag{A7}$$

The solution of this linear equation is

$$\begin{pmatrix} u_1 \\ v_1 \end{pmatrix} = \begin{pmatrix} 1 \\ \alpha \end{pmatrix} \tilde{A}(X,T) e^{ik_T x} + c.c., \tag{A8}$$

where

$$\alpha = k_T^2 (k_T^2 + 5)/20\zeta_2, \quad \tilde{A} = \varepsilon^{-1/2} A, \tag{A9}$$

which is consistent with Eq. (A1).

At order $|\varepsilon|$,

$$\mathcal{L} \begin{pmatrix} u_2 \\ v_2 \end{pmatrix} = \mathcal{M} \begin{pmatrix} u_1 \\ v_1 \end{pmatrix} - \begin{pmatrix} 4 \\ \sigma b_T \end{pmatrix} (v_1 \chi_1 - u_1 \chi_2) u_1 - \begin{pmatrix} -1 \\ \sigma b_T \end{pmatrix} \frac{2\gamma_1}{\pi} \cos(k_f x), \tag{A10}$$

where $\mathcal{M} = -2 \begin{pmatrix} 1 \\ d\sigma \end{pmatrix} \partial_x \partial_X$ and

$$\chi_1 = \frac{u_0^2 - 1}{(u_0^2+1)^2}, \quad \chi_2 = \frac{u_0 (u_0^2 - 3) v_0}{(u_0^2+1)^3}. \tag{A11}$$

In order for (u_2, v_2) to belong to the vector space of periodic functions, the right-hand side of Eq. (A10) should be orthogonal to the null space of $\mathcal{L}^\dagger$, the adjoint of $\mathcal{L}$. The adjoint operator is given by

$$\mathcal{L}^\dagger = \begin{pmatrix} 4\zeta_1 - 5 + \partial_x^2 & \sigma b_T \zeta_1 \\ -4\zeta_2 & -\sigma b_T \zeta_2 + d\sigma \partial_x^2 \end{pmatrix}, \tag{A12}$$

and its null space is spanned by

$$\mathbf{h}_\pm = \begin{pmatrix} -1 \\ 1/\alpha\sigma d \end{pmatrix} e^{\pm ik_T x}, \tag{A13}$$

that is, $\mathcal{L}^\dagger \mathbf{h}_\pm = 0$. It is straightforward to verify that the right-hand side of Eq. (A10) is indeed orthogonal to $\mathbf{h}_\pm$ and no solvability condition is needed at this order.

The solution at this order reads

$$\begin{pmatrix} u_2 \\ v_2 \end{pmatrix} = \begin{pmatrix} c_1 \\ c_2 \end{pmatrix} \tilde{A} e^{2ik_T x} + \begin{pmatrix} 0 \\ c_3 \end{pmatrix} |\tilde{A}|^2 - \begin{pmatrix} c_4 \\ c_5 \end{pmatrix} \frac{2\gamma_1}{\pi} e^{ik_f x} + \frac{1}{4\zeta_2} \begin{pmatrix} 0 \\ 1 \end{pmatrix} \mathcal{M} \tilde{A} e^{ik_T x} + c.c., \tag{A14}$$

where $c_3 = 2(\alpha\chi_1 - \chi_2)/\zeta_2$ and

$$\begin{pmatrix} c_1 \\ c_2 \end{pmatrix} = \frac{c_3}{9} \begin{pmatrix} 8\zeta_2/k_T^2 \\ (4k_T^2 + 5)/10 \end{pmatrix},$$

$$\begin{pmatrix} c_4 \\ c_5 \end{pmatrix} = \begin{pmatrix} \left(k_f^2 + k_T^4\right)/2\left(k_f^2 - k_T^2\right)^2 \\ k_T^4 \left(-4k_f^2 + k_T^4 + 10k_T^2 + 5\right)/40\zeta_2 \left(k_f^2 - k_T^2\right)^2 \end{pmatrix}. \tag{A15}$$

Finally, at order $|\varepsilon|^{3/2}$ we obtain

$$\mathcal{L}\begin{pmatrix} u_3 \\ v_3 \end{pmatrix} = \partial_T \begin{pmatrix} u_1 \\ v_1 \end{pmatrix} - \partial_X^2 \begin{pmatrix} u_1 \\ d\sigma v_1 \end{pmatrix} + \sigma b_T \begin{pmatrix} 0 \\ \zeta_1 u_1 - \zeta_2 v_1 \end{pmatrix} + \mathcal{M}\begin{pmatrix} u_2 \\ v_2 \end{pmatrix} + \begin{pmatrix} 4 \\ \sigma b_T \end{pmatrix} \times \left[\chi_2 \left(\frac{u_1^2 v_1}{v_0} + 2u_2 u_1 \right) - \chi_1 (u_2 v_1 + u_1 v_2) - \chi_3 u_1^3 \right], \tag{A16}$$

where

$$\chi_3 = \frac{\left(u_0^4 - 6u_0^2 + 1\right) v_0}{\left(u_0^2 + 1\right)^4}. \tag{A17}$$

Applying the solvability condition on the right-hand side of Eq. (A16), going back to the fast variables, and replacing the amplitude $\tilde{A}$ by

$$B = |\varepsilon|^{-1/2} \tilde{A} e^{i\nu_1 X}, \tag{A18}$$

we obtain the amplitude equation (10),

$$\tau \partial_t B = \mu B - \eta |B|^2 B + \Gamma B^\star + (\partial_x - i\nu)^2 B, \tag{A19}$$

where the coefficients that appear in the equation are

$$\tau = \frac{(d\sigma - 1)\left(k_T^2 + 5\right)}{20 d\sigma}, \quad \mu = \alpha \zeta_2 \left(1 - \frac{b}{b_T}\right),$$
$$\Gamma = \frac{2\gamma}{\pi} \left[c_4 (-\alpha \chi_1 + 2\chi_2) - c_5 \chi_1 \right],$$
$$\eta = -\chi_1 (\alpha c_1 + c_2 + c_3) + \chi_2 \left(2c_1 + \frac{3\alpha}{v_0} \right) - 3\chi_3. \tag{A20}$$

Note that both Γ and η are independent of b.

[1]R. Peter, M. Hilt, F. Ziebert, J. Bammert, C. Erlenkämper, N. Lorscheid, C. Weitenberg, A. Winter, M. Hammele, and W. Zimmermann, "Stripe-hexagon competition in forced pattern-forming systems with broken up-down symmetry," Phys. Rev. E **71**, 046212 (2005).
[2]G. Seiden, S. Weiss, J. H. McCoy, W. Pesch, and E. Bodenschatz, "Pattern forming system in the presence of different symmetry-breaking mechanisms," Phys. Rev. Lett. **101**, 214503 (2008).
[3]G. Freund, W. Pesch, and W. Zimmermann, "Rayleigh–Bénard convection in the presence of spatial temperature modulations," J. Fluid Mech. **673**, 318–348 (2011).
[4]M. Dolnik, T. Bánsági, S. Ansari, I. Valent, and I. R. Epstein, "Locking of Turing patterns in the chlorine dioxide–iodine–malonic acid reaction with one-dimensional spatial periodic forcing," Phys. Chem. Chem. Phys. **13**, 12578–12583 (2011).
[5]R. Manor, A. Hagberg, and E. Meron, "Wave-number locking in spatially forced pattern-forming systems," EPL **83**, 10005 (2008).
[6]Y. Mau, A. Hagberg, and E. Meron, "Spatial periodic forcing can displace patterns it is intended to control," Phys. Rev. Lett. **109**, 034102 (2012).
[7]R. Manor, A. Hagberg, and E. Meron, "Wavenumber locking and pattern formation in spatially forced systems," New J. Phys. **11**, 063016 (2009).
[8]M. Z. Hossain and J. M. Floryan, "Instabilities of natural convection in a periodically heated layer," J. Fluid Mech. **733**, 33–67 (2013).
[9]Y. Mau, L. Haim, A. Hagberg, and E. Meron, "Competing resonances in spatially forced pattern-forming systems," Phys. Rev. E **88**, 032917 (2013).
[10]S. Weiss, G. Seiden, and E. Bodenschatz, "Resonance patterns in spatially forced Rayleigh–Bénard convection," J. Fluid Mech. **756**, 293–308 (2014).
[11]L. Haim, Y. Mau, and E. Meron, "Spatial forcing of pattern-forming systems that lack inversion symmetry," Phys. Rev. E **90**, 022904 (2014).
[12]H.-C. Kao, C. Beaume, and E. Knobloch, "Spatial localization in heterogeneous systems," Phys. Rev. E **89**, 012903 (2014).
[13]Y. Mau, L. Haim, and E. Meron, "Reversing desertification as a spatial resonance problem," Phys. Rev. E **91**, 012903 (2015).
[14]H.-K. Park, "Frequency locking in spatially extended systems," Phys. Rev. Lett. **86**, 1130–1133 (2001).
[15]A. Yochelis, A. Hagberg, E. Meron, A. L. Lin, and H. L. Swinney, "Development of standing-wave labyrinthine patterns," SIAM J. Appl. Dyn. Syst. **1**, 236–247 (2002).
[16]A. Yochelis, C. Elphick, A. Hagberg, and E. Meron, "Two-phase resonant patterns in forced oscillatory systems: Boundaries, mechanisms and forms," Physica D **199**, 201–222 (2004).
[17]B. Marts, A. Hagberg, E. Meron, and A. L. Lin, "Bloch-front turbulence in a periodically forced Belousov-Zhabotinsky reaction," Phys. Rev. Lett. **93**, 108305 (2004).
[18]J. Burke, A. Yochelis, and E. Knobloch, "Classification of spatially localized oscillations in periodically forced dissipative systems," SIAM J. Appl. Dyn. Syst. **7**, 651–711 (2008).
[19]A. S. Mikhailov and K. Showalter, "Control of waves, patterns and turbulence in chemical systems," Phys. Rep. **425**, 79–194 (2006).
[20]P. Coullet, J. Lega, B. Houchmanzadeh, and J. Lajzerowicz, "Breaking chirality in nonequilibrium systems," Phys. Rev. Lett. **65**, 1352 (1990).
[21]C. Elphick, A. Hagberg, E. Meron, and B. Malomed, "On the origin of traveling pulses in bistable systems," Phys. Lett. A **230**, 33–37 (1997).
[22]I. V. Barashenkov and S. R. Woodford, "Complexes of stationary domain walls in the resonantly forced Ginsburg-Landau equation," Phys. Rev. E **71**, 026613 (2005).
[23]L. Korzinov, M. Rabinovich, and L. Tsimring, "Symmetry breaking in nonequilibrium systems: Interaction of defects," Phys. Rev. A **46**, 7601 (1992).
[24]L. Haim, A. Hagberg, R. Nagao, A. P. Steinberg, M. Dolnik, I. R. Epstein, and E. Meron, "Fronts and patterns in a spatially forced CDIMA reaction," Phys. Chem. Chem. Phys. **16**, 26137–26143 (2014).
[25]A. P. Muñuzuri, M. Dolnik, A. M. Zhabotinsky, and I. R. Epstein, "Control of the chlorine dioxide-iodine-malonic acid oscillating reaction by illumination," J. Am. Chem. Soc. **121**, 8065–8069 (1999).
[26]I. Lengyel, G. Rabai, and I. R. Epstein, "Experimental and modeling study of oscillations in the chlorine dioxide-iodine-malonic acid reaction," J. Am. Chem. Soc. **112**, 9104–9110 (1990).
[27]A. Hagberg and E. Meron, "The dynamics of curved fronts: Beyond geometry," Phys. Rev. Lett. **78**, 1166–1169 (1997).
[28]M. C. Cross and P. C. Hohenberg, "Pattern formation outside of equilibrium," Rev. Mod. Phys. **65**, 851 (1993).
[29]E. Meron, *Nonlinear Physics of Ecosystems* (CRC Press, Taylor & Francis Group, 2015).